Electrospinning Preparation and Photoluminescence Properties of Rare-Earth Complex/Polymer Composite Fibers

Hui Zhang, Hongwei Song,* Hongquan Yu, Xue Bai, Suwen Li, Guohui Pan, Qilin Dai, Tie Wang, Wenlian Li, Shaozhe Lu, Xinguang Ren, and Haifeng Zhao

Key Laboratory of Excited State Physics, Changchun Institute of Optics, Fine Mechanics and Physics, Chinese Academy of Sciences, 16 Eastern South-Lake Road, Changchun 130033, People's Republic of China and Graduate School of Chinese Academy of Sciences, Beijing 10039, People's Republic of China

Received: December 7, 2006; In Final Form: March 8, 2007

Composite fibers of poly(vinyl pyrrolidone) (PVP, $M_w \approx 1\,300\,000$) and europium complex $Eu(BA)_3(TPPO)_2$ (BA =1-benzoylacetone; TPPO = triphenylphosphine oxide) with strong photoluminescence were prepared by electrospinning. Their luminescent properties were studied in comparison to that of the pure complex. The results indicate that due to decreased symmetry in the composites the excitation bands are split into two different components, peaking at ~246 and ~336 nm, respectively, while the ratio of the electronic dipole $^5D_0$-$^7F_2$ transitions to the magnetic dipole $^5D_0$-$^7F_1$ ones in the emission spectra becomes a little larger. The room temperature fluorescence lifetime for the $^5D_0$ level becomes shorter due to increased radiative and nonradiative transition rates. The temperature dependence of photoluminescence was investigated under 325-nm excitation. It is interesting to observe that in the composite fiber the total emission intensity of the Eu^{3+} ions changes little below 150 K, while in the pure complex the intensity decreases monotonically with increasing temperature. In addition, the composite fibers exhibit better photostability exposed to ultraviolet lights. These novel luminescent composite fibers have potential application in nanodevices.

1. Introduction

One-dimensional (1D) nanostructural materials have gained considerable attention recently owing to their unique properties and intriguing applications in many areas.[1] 1D organic−inorganic composites are particularly challenging, because they could integrate the advantages of both the organic materials (flexibility, processability, and lightweight) and the inorganic materials (hardness, heat stability, chemical resistance, and optical function).[2] Electrospinning is a simple, versatile, and useful technique for fabricating nanofibers from a rich variety of functional materials that are exceptionally long in length and uniform in diameter. The diameters of fibers prepared by this method can range from tens of nanometers to several micrometers. The morphology of the electrospun fibers depends on the solvent and the solution properties, as well as other processing variables.[3]

Luminescent rare earth (RE) organic complexes are of both fundamental and technical interest due to their characteristic luminescence properties, such as extremely sharp emission bands, long lifetime, and potential high internal quantum efficiency. The rare earth complexes incorporated in the polymer matrix embody a class of new materials that present the characteristics of the complexes, making them applicable in a wide range of new technologies. The polymer-capped rare earth complexes are important because they possess the properties of the complexes while they can be processed from solution and are mechanically flexible.[4]

In this paper, $Eu(BA)_3(TPPO)_2$/PVP composite fibers with intense brightness were prepared through electrospinning. Their luminescent properties were studied in comparison with that of the relevant pure europium complex $Eu(BA)_3(TPPO)_2$. It is important to observe that the thermal stability and photostability of the luminescence in the composite fibers is improved over those of the pure europium complex.

2. Experimental Section

A. Sample Preparation. $Eu(BA)_3(TPPO)_2$ was synthesized according to the traditional method.[5] In the preparation, an appropriate amount of PVP was dissolved in ethanol at a concentration of 7, 9, 12 and 14 wt %, respectively. After stirring, appropriate amounts of $Eu(BA)_3(TPPO)_2$ with the same weight were dissolved into the same volume prepared PVP ethanol solutions, which were stirred to be uniform. The final solution then was electrospun to give composite fibers of $Eu(BA)_3(TPPO)_2$ complex and PVP. The schematic diagram of the electrospinning setup was shown in Figure 1. It consists of three major components: a high-voltage power supply, a spinneret (a needle), and a collector plate (a grounded conductor). The voltage used for electrospinning was 14 kV, and the collection distance was 30 cm. In the following text, the pure $Eu(BA)_3(TPPO)_2$ complex and $Eu(BA)_3(TPPO)_2$/PVP composite fibers electrospun from 7, 9, 12 and 14 wt % concentration of PVP ethanol solution are labeled as samples A, B, C, D, and E, respectively. The mass ratio of the $Eu(BA)_3(TPPO)_2$ complex to PVP in samples B, C, D, and E was calculated to be ~1:23, 1:30, 1:40, and 1:47, respectively.

B. Measurements. The size and morphology of the composite fibers were obtained by using a S-4800 scanning electron microscope (Hitachi). The excitation and emission spectra were recorded at room temperature with a Hitachi F-4500 spectrophotometer equipped with a continuous 150-W Xe-arc lamp. In the experiments of spectral change induced by UV light

* Address correspondence to this author. E-mail: hwsong2005@yahoo.com.cn. Fax: 86-431-86176320.

10.1021/jp0684123 CCC: $37.00
Published on Web 04/11/2007

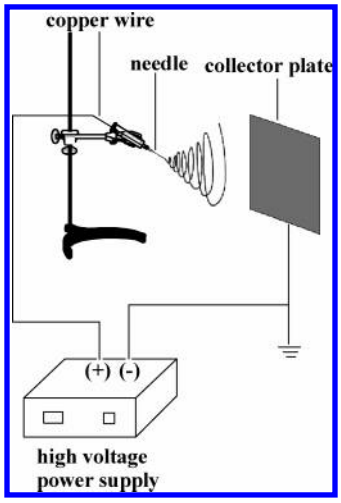

Figure 1. Schematic diagram of the electrospinning setup.

irradiation, the monochromic light separated from the same Xe-arc lamp was used as the irradiation source, with a slit of 10 nm. In the measurements of temperature dependence of fluorescence the samples were placed into a liquid nitrogen cycling system (pellet). A continuous 325-nm light from a He−Cd laser was used as the excitation source. The fluorescence was measured by a UV-Lab Raman Infinity (made by Jobin Yvon Company) with a resolution of 2 cm^{-1}. In the measurements of fluorescence dynamics, a 355-nm light generated from a Nd^{3+}:YAG (yttrium aluminum garnet) laser combined with a third-harmonic generator was used as the pump. An oscillograph was used to record the decay dynamics.

3. Results and Discussion

A. Characterization. Figure 2a−d shows the scanning electron microscope (SEM) image of composite fiber samples B, C, D, and E, respectively. From Figure 2e we can see that uniform and super-long nanowires are formed in sample B, with lengths of several tens to hundreds micrometers. The composite fibers in the other samples yield similar lengths. The average diameters for samples B, C, D, and E are ~200, 350, 500, and 700 nm, respectively. Apparently, the diameters of the composite fibers increase with the increase of PVP concentration.

Figure 3 shows the Fourier transform infrared (FTIR) spectra of the different samples. The $Eu(BA)_3(TPPO)_2$ complex used to fabricate the composite fibers is a kind of nonhydrated complex, which can be proven by the absence of the O−H stretching mode in the IR absorption spectrum for the pure $Eu(BA)_3(TPPO)_2$ complex. The composite fibers contain a trace hydroxyl group due to the electrospun solution. A broad band at 3400 cm^{-1} appears in the composite fibers, which is assigned to vibration of the associated hydroxyl groups. The FTIR spectra of the composite fibers are similar to that of the PVP fibers electrospun from the PVP ethanol solution, suggesting that the europium complexes are capped in the PVP matrix in the composite fibers.

B. Excitation and Emission Spectra. The photoluminescence properties of the composite fibers were studied and compared with that of the pure europium complex. Figure 4 shows the excitation and emission spectra of various samples. In the pure complex, a broad excitation band extending from 200 to 400 nm appears, which is assigned to the $\pi-\pi^*$ electron transition of the ligands. In the composite, it is interesting to observe that the excitation band is split into two components, having peaks at ~246 and ~336 nm, respectively. This indicates

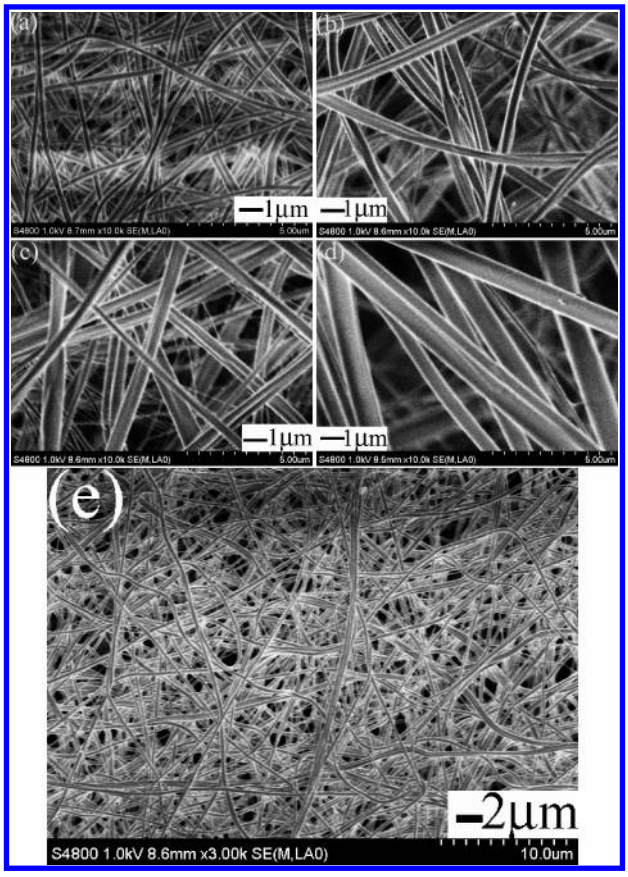

Figure 2. SEM images of $Eu(BA)_3(TPPO)_2$/PVP composite fibers: (a) sample B, (b) sample C, (c) sample D, (d) sample E, and (e) image for sample B on a large scale.

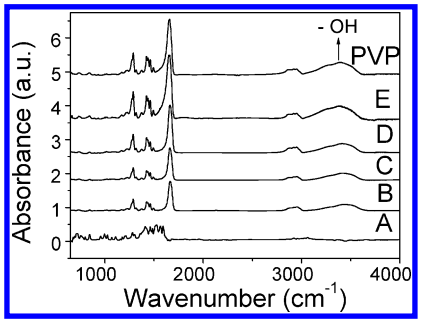

Figure 3. Infrared absorption spectra of the pure $Eu(BA)_3(TPPO)_2$ complex (A), the $Eu(BA)_3(TPPO)_2$/PVP composite fibers (B, C, D, and E), and the pure PVP fibers.

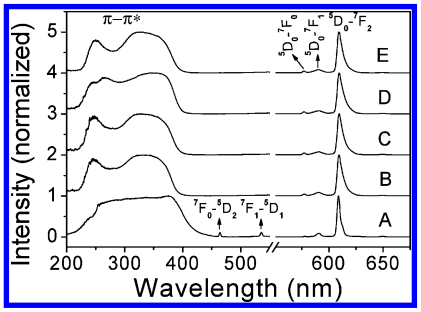

Figure 4. Excitation spectra (λ_{em} = 609 nm) and emission spectra (λ_{ex} = 331 nm) of different samples.

that in the composite due to the existence of the surrounding PVP media, the site symmetry becomes lower.[6] In addition, in the excitation spectrum of the pure complex the $^7F_0$-$^5D_2$ and $^7F_1$-$^5D_1$ excitation lines appear, while in the composites the lines disappear. This suggests that in the composites the f−f inner-

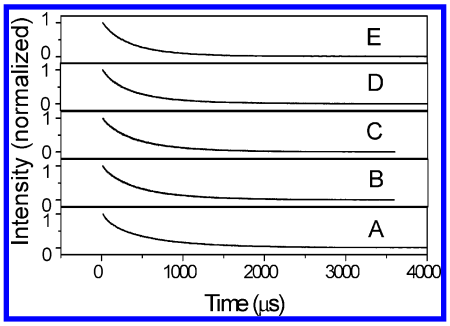

Figure 5. Fluorescence decay dynamics of the $^5D_0$-$^7F_2$ transitions (λ_{em} = 609 nm) in various samples (room temperature).

shell transitions are quenched through the nonradiative energy transfer from the higher excited states to some uncertain defect levels, substituting for the nonradiative relaxation to $^5D_0$.

In the emission spectra, the red $^5D_0$-^7F_J (J = 0, 1, 2) transitions are clearly observed. They demonstrate two features for the spectral properties of Eu^{3+} ions in the composites: (1) The emission lines in the composites become broader over the pure complex, which is attributed to heterogeneous broadening caused by more disordered local environments surrounding Eu^{3+} ions. (2) The intensity ratio of $^5D_0$-$^7F_2$ to $^5D_0$-$^7F_1$ in the composite fibers increases a little over the pure complex. The ratios in samples A, B, C, D, and E are determined to be 7.8, 8.5, 9.3, 9.4, and 9.0, respectively. As is well-known, the magnetic dipole transitions $^5D_0$-$^7F_1$ are largely independent of the ligand field and therefore can be used as an internal standard to account for the ligand differences.[7] The electric dipole transitions $^5D_0$-$^7F_2$, so-called hypersensitive transitions, are sensitive to the symmetry of the coordination sphere. The intensity ratio of the magnetic dipole transition to the electric dipole transition in the lanthanide complex measures the symmetry of the coordination sphere.[8] Therefore, the above results indicate that the presence of PVP generally increases the luminescent intensity of the hypersensitive transitions of the lanthanide ions. When the europium complexes are incorporated into the microcavities of the PVP matrix, the complexes exhibit more disordered local environments due to the influence of the surrounding PVP. Under the influences of the electric field of the surrounding ligands, the distortion of the symmetry around the lanthanide ions by the capping PVP results in the polarization of the Eu^{3+}, which increases the probability for electronic dipole allowed transitions. A similar increase of the relative intensity of $^5D_0$-$^7F_2$ to $^5D_0$-$^7F_1$ was also observed in the europium complex incorporated in the PVP matrix.[4] Here, no effort was made to compare the absolute luminescent intensities of the complexes in the presence or absence of PVP since the number of molecules in the excitation beam was unequal. However, what we can claim is that the brightness for the composites is very intense, although the concentration of the europium complex in the samples is quite small.

C. Fluorescence Dynamics. The fluorescence decay curves of $^5D_0$-$^7F_2$ emissions for Eu^{3+} ions under 355-nm excitation were measured at room temperature, as shown in Figure 5. It can be seen that the fluorescence decays exponentially for all the samples. The exponential lifetimes for the $^5D_0$ states are obtained to be 573 μs in sample A, 484 μs in sample B, 467 μs in sample C, 429 μs in sample D, and 409 μs in sample E. It is obvious that the fluorescence lifetime for the $^5D_0$ state in the composite fibers becomes shorter than that in the pure europium complex.

In fact, the lifetime of $^5D_0$, τ is dominated by the total radiative transition rate of $^5D_0$-Σ^7F_J, W_r, and the nonradiative decay rate W_{nr}, which can be written as $\tau = 1/(W_r + W_{nr})$. W_{nr} includes the nonradiative relaxation rate from $^5D_0$ to lower ^7F_J levels and the nonradiative energy transfer rate to the other defect centers. In the composite, due to the increased electronic dipole transition caused by incorporation of PVP, the total radiative transition rate of $^5D_0$-Σ^7F_J should increase, which may be one factor leading to the shortening of fluorescence lifetime.

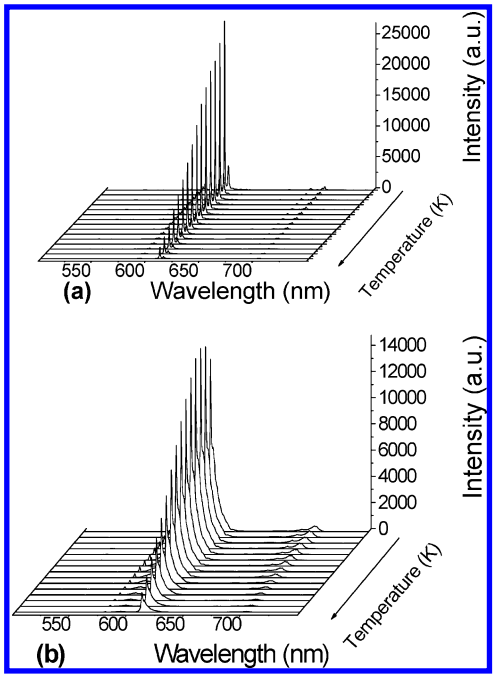

Figure 6. Emission spectra at various temperatures under 325-nm excitation.

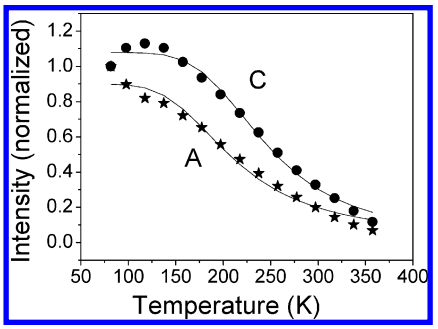

Figure 7. Dependence of emission intensity of the Σ^5D_0-^7F_J transitions on temperature: (a) $Eu(BA)_3(TPPO)_2$ complex and (b) $Eu(BA)_3$-$(TPPO)_2$/PVP.

The nonradiative relaxations in the rare earth complexes are governed by the energy difference between the emitting level and the next lower level, separated by the number of phonons of the host.[9] In the composite fiber samples the hydroxyl groups with large phonon energy may lead to an increase of the nonradiative transition rate from $^5D_0$ to ^7F_J according to the theory of multiphonon relaxation. We suggest that the increased nonradiative transition rate is the main factor leading to the shortening of fluorescence lifetime.

D. Temperature Dependence of Emission Intensity. To study the thermal stability of photoluminescence, the temperature dependence of fluorescence intensity was measured under 325-nm excitation in various samples. Parts a and b of Figure 6 display the emission spectra of the pure europium complex and the composite fiber sample C at different temperatures, respectively. The corresponding dependence of emission intensity of the $^5D_0$-$^7F_2$ on temperature was drawn as Figure 7. It is obvious that the variation of the emission intensity for the Eu^{3+} ions in the composite fiber shows a remarkable difference

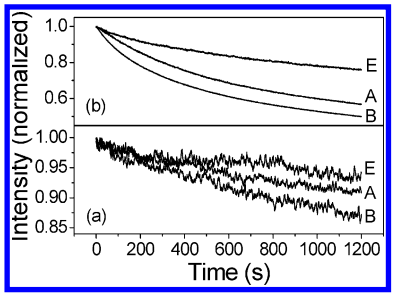

Figure 8. Dependence of normalized intensity at 609 nm on irradiation time in different samples. The samples are irradiated by (a) 245- and (b) 331-nm light.

related to that in the pure complex. The emission intensity of the pure $Eu(BA)_3(TPPO)_2$ complex powder decreases monotonically with the increasing temperature in the studied range. In the $Eu(BA)_3(TPPO)_2$/PVP composite fiber the total emission intensity of the Eu^{3+} ions changes little below 150 K, then it decreases quickly as temperature increases continuously. The intensity as a function of temperature can be well fitted by the well-known thermal activation function[10]

$$I(T) = I/(1 + \alpha \exp(-E_A/K_BT))$$

where I_0 is the emission intensity at 0 K, α is the proportional coefficient, E_A is the thermal activation energy, K_B is Boltzmann's constant, and T is the absolute temperature. The values of E_A in samples A and C are respectively 84.1 and 117.1 meV. The improved value of E_A in the composite fiber suggests that the thermal stability of the photoluminescence is better than that in the pure complexes. The other composite fiber samples are similar with sample C in temperature dependence.

It is well-known that in RE complexes energy is transferred from the triplet state of ligands to the center RE ions, which raises the 4f electron of the RE ions to excited energy levels. Radiative electronic transitions back to the ground state or to other lower states give off photons. Due to the shielding effect of electrons in the outer shells, inner 4f electronic transitions of the RE ions give rise to a narrow emission band, which is insensitive to the chemical environment. The sensitization pathway in luminescent rare earth complexes generally consists of an initial strong absorption of ultraviolet energy that excites the ligand to the excited singlet (S_1) state, followed by an energy migration via intersystem crossing from the S_1 state to a ligand triplet (T) state. The energy is then nonradiatively transferred from the lowest triplet state of the ligand to a resonance state of a coordinated lanthanide ion, which in turn undergoes a multiphoton relaxation and subsequent emission in the visible region.[11,12] The intramolecular energy migration efficiency from organic ligands to the central Eu^{3+} ions is the most important factor influencing the luminescent properties of the RE complexes. We suggest that in the composite fibers due to the existence of PVP matrix, the energy transfer from one excited Eu^{3+} ion to the other Eu^{3+} ions is decreased and the vibrational transitions of the complexes are restrained, leading to improved thermal stability of photoluminescence.[4]

E. Photoluminescence Stability. To compare the photoluminescence stability, ultraviolet light irradiation induced spectral changes in different samples were also studied. Figure 8 shows the dependence of normalized emission intensity at 609 nm on irradiation time in different samples. It is clear that in the composites, as the PVP concentration in the composite fiber is lower, the relative change is larger than that in the pure complex. As the PVP concentration is high enough, the relative change in the composite fiber is smaller than that in the pure complex, indicating better photoluminescence stability. This indicates that low PVP concentration is not effective in stabilizing the europium complex.

4. Conclusions

In summary, uniform and superlong $Eu(BA)_3(TPPO)_2$/PVP composite fibers were prepared by electrospinning, which demonstrated intense photoluminescence under ultraviolet excitation. The diameters of the composite fibers were adjusted in the range of 200−1000 nm by changing the concentration of PVP ethanol solution. The luminescent properties of the composite fibers were studied and compared to those of the pure complex $Eu(BA)_3(TPPO)_2$. The results demonstrate that due to the degeneration of crystal field and more disordered local environments, the excitation bands are split into different components, while the ratio of electronic dipole transitions of $^5D_0$-$^7F_2$ to the magnetic dipole transition of $^5D_0$-$^7F_1$ increases due to increased electronic dipole transition probabilities. In addition, the fluorescence decay time constants for the $^5D_0$-$^7F_2$ transitions become shorter because of increased radiative and nonradiative transition rates. Most importantly, in the composite fibers the temperature stability and photostability of the luminescence become better in comparison to those of the pure complex due to the modification by PVP matrix.

Acknowledgment. The authors thank the National Natural Science Foundation of China (Grants 10374086 and 10504030) and the Talent Youth Foundation of JiLin Province (Grants 20040105) for financial. They also thank Liangliang Han for help in the preparation of the pure europium complex.

References and Notes

(1) (a) Xia, Y.; Yang, P.; Sun, Y.; Wu, Y.; Mayers, B.; Gates, B.; Yin, Y.; Kim, F.; Yan, H. *Adv. Mater.* **2003**, *15*, 353. (b) Hu, J.; Odom, T. W.; Lieber, C. M. *Acc. Chem. Res.* **1999**, *32*, 435.

(2) Sui, X.; Shao, C.; Liu, Y. *Appl. Phys. Lett.* **2005**, *87*, 113115.

(3) Deitzel, J. M.; Kleinmeyer, J.; Harris, D.; Tan, N. C. B. *Polymer* **2001**, *42*, 261.

(4) Li, Q.; Li, T.; Wu, J. *J. Phys. Chem. B* **2001**, *105*, 12293.

(5) Melby, L. R.; Rose, N. J.; Abramson, E.; Caris, J. C. *J. Am. Chem. Soc.* **1964**, *86*, 5117.

(6) Chang, N. C.; Gruber, J. B. *J. Chem. Phys.* **1964**, *41*, 3227.

(7) Bunzli, J.-C. G. Luminescent Probes. In *Lanthanide probes in Life, Chemical and Earth Sciences*, *Theory and Practice*; Bunzli, J.-C. G., Choppin, G. R., Eds.; Elsevier: New York, 1989; p 219.

(8) Kirby, A. F.; Foster, D.; Richardson, F. S. *Chem. Phys. Lett.* **1983**, *95*, 507.

(9) Reisfeld, R. *Mater. Sci.* ***2002****, 20, 5.*

(10) Li, B. S.; Liu, Y. C.; Zhi, Z. Z.; Shen, D. Z.; Lu, Y. M.; Zhang, J. Y.; Fan, X. W. *J. Cryst. Growth* **2002**, *240*, 479.

(11) Tanaka, M.; Yamagughi, G.; Shiokawam, J.; Yamanaka, C. *Bull. Chem. Soc. Jpn.* **1970**, *43*, 549.

(12) Haynes, A. V.; Drickamer, H. G. *J. Chem. Phys.* **1982**, *76*, 114.